J. Biochem. **140**, 185–191 (2006)
doi:10.1093/jb/mvj150

Prompt Non-Stacking Binding of Actinomycin D to Hairpin Oligonucleotide HP1 and Slow Redistribution from HP1 to DNA

Nikolai Vekshin* and Alexander Kovalev
Institute of Cell Biophysics, Pushchino, Moscow region, 142290, Russia

Received May 7, 2006; accepted May 19, 2006

Complexes of actinomycin D (AMD) and 7-amino-actinomycin D (7AAMD) with model hairpin oligonucleotide HP1 and various types of DNA in aqueous solutions were investigated by steady-state, polarized, time-resolved and stopped-flow fluorimetry, and photometry. Prompt non-stacking binding of the actinomycins inside HP1 was observed. No energy transfer from nucleotides to 7AAMD in the complex was detected, most likely because of the absence of stacking intercalation. Complex formation of AMD or 7AAMD and HP1 was followed by the transition from a random flexible conformation of the hairpin to a more compact rigid structure, and subsequently to hypochromism. Strong competition between AMD and 7AAMD for a cavity in HP1 was observed. The decrease in the 7AAMD emission after addition of DNA to the 7AAMD/HP1 complex indicates that actinomycins can be redistributed from HP1 to DNA, *i.e.* hairpin oligonucleotides can serve as molecular carriers of actinomycins.

Key words: actinomycin D, 7-amino-actinomycin D, DNA, energy transfer, fluorescence, hairpin oligonucleotide, non-stacking binding, stopped-flow.

Abbreviations: AMD, actinomycin D; 7AAMD, 7-amino-actinomycin D; HP1, hairpin oligonucleotide; λDNA, lambda DNA; EB, ethidium bromide.

Actinomycins are widely applied because of their antibiotic and anti-tumour activity. They are still used for the treatment of different types of cancers like rhabdomiosarcomas, genital malignancies, *etc.* (*1–4*). Moreover, actinomycins decelerate ageing by prolonging the life cycle (*5*). Well known among actinomycins is actinomycin D (AMD), consisting of 2-aminophenoxazin-3-one chromophore and two cyclic pentapeptide lactones. The biological activity of AMD is attributed to its ability to bind to DNA, and thus to inhibit the RNA polymerase reaction and protein biosynthesis (*6–8*). AMD is biologically active at low concentrations. At high concentrations, AMD has a toxic effect.

The widespread application of AMD requires determination the molecular mechanism of the AMD/DNA complex formation. It is generally accepted, that AMD intercalates into duplex DNA, preferring GpC sites (*6*, *9*). An alternative binding mechanism at non-GpC (*i.e.* ApT/TpA) sites is also possible (*10*). In the solid phase, the stacking intercalation of phenoxazone chromophore between nucleotides was shown in crystals by X-ray analysis (*9*) and in films by fluorescence energy transfer (*11*). In aqueous solutions, actinomycins can bind to DNA in two ways: (a) stacking-like intercalation, at high concentrations, and (b) binding in non-stacking positions, at low concentrations (*11*, *12*). The highest binding constant for actinomycins was observed for hairpin-like sites or loops (*11–15*).

Instead of AMD, a fluorescent analog, 7-amino-actinomycin D (7AAMD), is usually used at low concentrations to study the properties of actinomycin/DNA complexes (*11–17*). The excitation spectrum of this dye bound to DNA exhibits a long-wavelength ("red") shift in comparison to free 7AAMD in water, whereas the emission spectrum shows a short-wavelength ("blue") shift (*12*, *13*). The biggest difference in the fluorescence intensity of 7AAMD in DNA *vs.* 7AAMD in water was found on the "red-edge" of excitation and "blue-edge" of emission (*12*).

It has been shown that 7AAMD can form a compact complex with hairpin (single-stranded) oligonucleotides, with high binding constants (*14*, *15*, *17*). In particular, 7AAMD binds strongly to the 8.6-kDa hairpin HP1 d(5′-AAAAAAATAGTTTTAAATATTTTTTT-3′). The binding is accompanied by an increase by more than an order of magnitude in the fluorescence intensity due to changes in the lifetime and spectral shifts (*12*, *14–16*). The sequence of HP1 is also compatible with the formation of a homo-dimer, a mismatched duplex. In principle, hairpins can form both types of structures (they can be distinguished by native PAGE).

In (*12–17*) it was shown that at very low (physiological) concentrations (1 μM and lower) actinomycins can bind to hairpin oligonucleotides and to hairpin-like sites or loops in DNA. The highest binding constant was $\sim 10^7$ M^{-1} (*17*). However, the reason for such a strong interaction was unknown. It was also unclear why the binding takes place at a non-stacking position (*11, 12*). It is important to determine the features of AMD and 7AAMD binding to HP1 and DNA at low concentrations. Also, it would be interesting to examine the possibility that actinomycins can be redistributed from HP1 to DNA. Such redistribution can be used in medicine for effective transport of antibiotics to DNA. That is why we performed the present spectroscopic investigation. The advantage of the present investigation over the previous ones is the combination of methods: steady-state, polarized, phase-modulating and

*To whom correspondence should be addressed. Phone: +8-27-73-94-32, Fax: +8-967-33-05-09, E-mail: nvekshin@rambler.ru

stopped-flow fluorimetry. Also, a new approach for determining the location and orientation of 7AAMD in HP1 and DNA by means of the efficiency of energy transfer (using excitation spectra) will be applied.

Prompt non-stacking interaction of actinomycins with HP1 will be described here. Strong competition between AMD and 7AAMD for the binding site inside HP1 will also be shown. Our data confirm the non-stacking binding of 7AAMD or AMD to HP1 in aqueous solutions. The results will be rationalized by means of a strong interaction between actinomycins and HP1, followed by transition from a random flexible conformation of the hairpin to a more compact rigid structure. It will be shown that 7AAMD or AMD can be transferred from HP1 to DNA. The biological significance of this finding is that hairpin oligonucleotides can serve as molecular carriers, transferring actinomycins to DNA.

MATERIALS AND METHODS

Actinomycin D ("Reanal"), 7-amino-actinomycin D ("Fluka"), oligonucleotide HP1 ("Midland Certified Reagent Company"), ethidium bromide ("Reachim"), Hoechst trihydrochloride (No. 33342, "Sigma"), calf thymus DNA ("Serva"), salmon sperm DNA (No. 101500, "ICN"), and lambda DNA (λDNA, No. 25250-010, "GibcoBRL") were used in this work. DNA and HP1 were dissolved in a buffer of low ionic strength (10 mM cacodylate or 10–20 mM Tris-HCl, pH 7.6).

Absorption spectra were measured with "M-40" (Carl Zeiss Jena, Germany) and "Cary" (Varian Analytical Instruments, Australia) spectrophotometers in 0.1-cm and 1-cm quartz cuvettes. The extinction coefficients (ε) are 13,000 M^{-1} cm^{-1} at 286 nm for ethidium, 24,500 M^{-1} cm^{-1} at 440 nm for AMD, and 12,600 M^{-1} cm^{-1} at 260 nm per nucleotide for DNA.

Fast association-dissociation kinetics of binding of 7AAMD to DNA or HP1 were detected at 26°C on the ms/s time scale by means of a stopped-flow fluorimeter "Applied Photophysics" (UK) with excitation at 550 nm and emission at >570 nm. Slow kinetics were detected in the minute time range with standard spectrofluorimeters, with excitation at 570 nm and emission at 610 nm in a 1-cm quartz cuvette. Mixed solutions were mechanically stirred. The slow emission kinetics were detected starting from 6 s after mixing. Kinetics evaluation data were processed using Matlab 4.0 software (MathWorks, Inc.), with fitting by least-squares methods (Gauss-Newton approximation).

Emission spectra of the 7AAMD/DNA and 7AAMD/HP1 complexes were recorded with a Perkin-Elmer MPF 44B spectrofluorimeter in a 0.4-cm quartz micro-cuvette. Corrected excitation spectra were recorded in the "ratio" regime.

Total efficiency (Q_{da}) of energy transfer from nucleotides to dye molecules was calculated with the equation (*18*, *19*):

$$Q_{da} = F_d\varepsilon_a[a]/F_a\varepsilon_d[d]$$

where ε_d is the extinction coefficient of the donor (in our case, it is the average ε of the nucleotides at 260 nm), ε_a is the extinction coefficient of the acceptor at its absorption maximum, [d] is the concentration of the donor, [a] is the concentration of the acceptor (the average concentration of nucleotides), F_d is the intensity of the donor band in the excitation spectrum (F_d equals the difference between the total intensity at 260 nm and the contribution from the acceptor at this wavelength), and F_a is the intensity of the acceptor band (F_a equals the total intensity at the acceptor excitation maximum minus the contribution from nucleotides at the same wavelength).

The number of nucleotides (N), donating the energy per one acceptor molecule, was estimated according to the equation:

$$N = F_d\varepsilon_a/F_a\varepsilon_d$$

Polarized emission of 7AAMD was measured with a SLM-4800 spectrofluorimeter (SLM Inc., US). The fluorescence lifetime was determined with phase-modulation techniques (using SLM; the modulation frequency was 30 MHz). The lifetime experiments were carried out in mirror micro-cuvettes, which highly increase the fluorescence signal (*19*).

The effective volume of the 7AAMD/DNA complex was calculated according to the Levshin-Perrin relationship (*19*):

$$1/P - 1/3 = (1/P_0 - 1/3)(1 + RT\tau/\eta V)$$

were P is the measured polarization, P_0 is the limit polarization = 0.5, R is the Rydberg's constant, T is the absolute temperature in K, τ is the lifetime, V is the effective volume of a particle, and η is the solvent viscosity (0.01 poise for aqueous solutions).

RESULTS AND DISCUSSION

Hypochromism Induced in HP1 by Actinomycins—The purpose of an absorption study is to obtain information about actinomycin-HP1 interactions and conformational properties of the complex. Complex formation between HP1 and 7AAMD or AMD leads to a considerable hypochromic effect on the 260-nm band of HP1 (Fig. 1): the optical density of the complex (curve 1) is sufficiently lower than the sum of curves 2 (HP1 only) and 3 (7AAMD only) in the UV region. In the visible region, only a small red shift without significant hypochromism for the actinomycin band was detected. The hypochromic value was not constant along the UV band (Table 1). Most hypochromism was observed at the edges of the band, but not at the maximum. This means that a strong exciton interaction between 7AAMD and HP1 takes place. The hypochromic values for AMD/HP1 differ only a little from those for 7AAMD/HP1. Consequently, AMD and 7AAMD bind to HP1 in a similar way.

The 260-nm absorption transition for nucleotides occurs in the chromophore plane. In native DNA, considerable stacking between nucleotides takes place. That is why the nucleotide ε in single-stranded DNA is sufficiently larger compared to that of the native DNA. Hypochromism is a result of a decrease in the absorption cross-section of chromophores in stacking-like structures (*20*). This arises due to exciton interactions and a screening effect (*19*, *20*). Hypochromism, induced in HP1 by AMD or 7AAMD, can be explained as a result of a transition of HP1 from a random flexible conformation to a more compact regular structure, where better stacking between nucleotides (but not

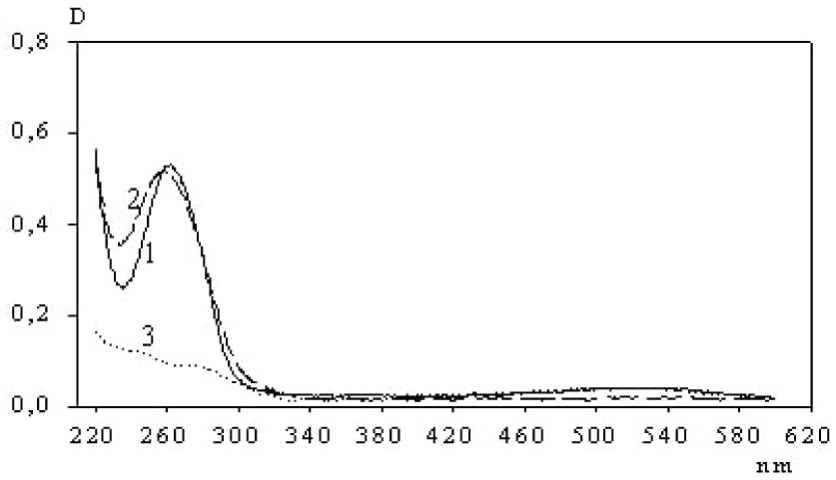

Fig. 1. **Absorption spectra of the 7AAMD/HP1 complex (1), HP1 (2), and 7AAMD (3).** The concentrations were: HP1 1.8 μM, and 7AAMD 2 μM. The buffer was 10 mM cacodylate (pH 7.6).

Table 1. **Hypochromism in the AMD/HP1 and 7AAMD/HP1 complexes.**[a]

Wavelength (nm)	Hypochromism (%) in AMD/HP1 complex	Hypochromism (%) in 7AAMD/HP1 complex
240	27	58
260	9	13
280	30	30
285	40	47

[a]The concentrations of AMD and 7AAMD were 2 μM, HP1 1.8 μM.

Table 2. **Fluorescence intensity of 7AAMD in the presence of various nucleic acids.**[a]

Sample	Intensity (rel.un.)
HP1 + 7AAMD	2,610
HP1 + 7AAMD + 10 μM AMD	160
HP1A + 7AAMD	250
Salmon sperm DNA + 7AAMD	740
Calf thymus DNA + 7AAMD	560
Lambda DNA + 7AAMD	505
Lambda DNA + 7AAMD + 80 μM AMD	205
Yeast t-RNA + 7AAMD	200
Buffer + 7AAMD	130

[a]The 7AAMD concentration was 1 μM. The buffer was 20 mM Tris-HCl (pH 7.5). The concentration of all types of DNA, yeast t-RNA, HP1 and HP1A was 0.014 mg/ml. Excitation was at 570 nm and emission was at 610 nm. The presented intensity values are the averages of five measurements.

stacking with the actinomycin chromophore) arises, when AMD or 7AAMD binds inside a dynamic "cavity" in HP1. This interpretation is in agreement with other data (*14*, *15*) concerning the greater thermal stability of the 7AAMD/HP1 or AMD/HP1 complex compared to the denaturized-like state of free HP1.

Fluorescent Properties of 7AAMD in Oligonucleotides and Nucleic Acids—Fluorescence is much more sensitive than absorption. That is why 7AAMD instead of AMD is used. In the case of the 7AAMD/HP1 complex, the intensity of the 7AAMD fluorescence is very high. The reasons for this are not only increases in the lifetime and quantum yield of 7AAMD after binding to the hairpin, but also a red shift in the 7AAMD excitation band (see excitation spectra in Refs. *11* and *12*). Besides, a blue shift of the emission band takes place (see emission spectra in Refs. *11–16*).

Replacing guanine in HP1 with adenine (HP1A) leads to an abrupt decrease in the binding affinity for actinomycins (Table 2). The presence of guanine in HP1 is essential for formation of the hairpin-like structure. This is why the presence of guanine nucleotide in HP1 is essential for 7AAMD binding. It is important to emphasize that there is no "specific interaction" between guanine and 7AAMD. Guanine itself is not an obligatory basis for binding of actinomycins (*10–12*, *21*). In fact, 7AAMD and AMD can effectively interact with oligonucleotides independently of the presence or absence of a GpC sequence (*10, 21*).

The lifetime of 7AAMD in the complex with HP1 was 1.7 ns. In the case of complexes with DNA, the 7AAMD lifetime was similar: 1.5–2.1 ns for all types of DNA used. However, the fluorescence intensity of 7AAMD in HP1 was 4–5 times higher than that in DNA (under the same conditions, Table 2). This means that the population of 7AAMD molecules in DNA is quenched. It can be suggested that such static quenching of 7AAMD takes place in the double helix by neighboring nucleotides (it is well known that nucleotides are strong quenchers, since they have very intense vibration modes).

The fluorescence intensity of 7AAMD depends on the type of DNA to which it is bound. Table 2 presents our data for lambda, calf thymus, and salmon sperm DNA. The fluorescence of 7AAMD reaches a plateau in 5 min after addition of the DNA aliquot. The highest 7AAMD emission intensity was observed for salmon sperm DNA, indicating that this DNA preparation contains many hairpin-like sites or loops and breaks. Relatively short λDNA has a minimum of hairpin-like sites and breaks. The hairpin-like sites, loops and breaks appear in the long double helix due to mechanical damage and thermal fluctuations.

In the presence of yeast t-RNA, the fluorescence intensity of 7AAMD was almost the same as in the case of free 7AAMD. Thus, 7AAMD is unable to bind to yeast t-RNA, since this rigid poly-nucleotide has too small a hairpin cavity. This means that the existence of hairpin-like sites itself is not sufficient for effective binding. Other

conditions are the size of a cavity or loop and flexibility of oligonucleotide tails. The free ends of the HP1 hairpin exhibit a high flexibility. Actinomycins can easily penetrate into open dynamically arising cavities inside a flexible hairpin structure. In the case of DNA, long loops and big hairpin-like sites are necessary for the fast actinomycin binding. The 7AAMD fluorescence intensity depends on the presence of hydrophobic cavities in the DNA structure.

Absence of Energy Transfer from Nucleotides to 7AAMD—Energy transfer from photo-excited nucleotides to a dye is one of the main features, indicating stacking intercalation in complexes (*19*, *22*). The stacking position of a dye between nucleotide chromophores in DNA provides a favourable condition for effective energy transfer. Energy transfer can be detected, for instance, as the appearance of the nucleotide band in the excitation spectrum of the emitting dye (*18*, *19*, *22*). The intercalating ability of 7AAMD in comparison with those of ethidium bromide (EB), a typical intercalating dye, and Hoechst 33342, a typical non-intercalating dye, was estimated here. EB induces denaturation and hyperchromism of native DNA (*19*). That is why EB is a strong cancer-inducing agent. On the contrary, Hoechst (for instance, H33342 and H33258) induces DNA condensation (*23*). It is interesting that Hoechst is known as an anticancer drug (*23*).

In the UV region, EB exhibits an intensive absorption band at 284 nm, Hoechst one at 340 nm, and 7AAMD one at 260 nm. The absorption band of EB overlaps to some degree with the nucleotide emission spectrum. The fluorescence quantum yield of poly-nucleotides in aqueous solutions at room temperatures is very low (*19*, *22*). Thus, Dexter's exchange energy transfer (*22*) from nucleotides to this dye could be expected only in the case of EB intercalation into DNA. Förster's dipole-dipole energy transfer (*22*) can hardly be expected here. The Hoechst absorption band overlaps sufficiently with the nucleotide emission spectrum. Therefore, both types of energy transfer could take place for Hoechst. In the case of 7AAMD, mainly Dexter's energy transfer can occur. To determine the efficiency of the total energy transfer, it is necessary to determine the fluorescence intensity of a dye, sensitized by nucleotides, and the intensity of a directly excited dye (it is also necessary to determine the nucleotide/dye relationship and absorbance) (*19, 22*).

The fluorescence intensity of EB increases after its binding to DNA. A strong nucleotide band at 260 nm was detected in the excitation spectrum of EB in DNA (*12, 19*). The same observation was made for EB in HP1 (*11, 12*). Hence, effective energy transfer takes place, which indicates stacking-like intercalation of EB. The nucleotide band in the EB excitation spectrum appears due to exchange energy transfer to EB from 1–2 neighbouring nucleotides (*12*, *18*, *19*). The calculated number of nucleotides (N) donating the excitation energy per one dye molecule in HP1 for the EB/HP1 complex is 1 (Table 3), *i.e.* one nucleotide donates the energy to one dye molecule. The efficiency (Q_{da}) of energy transfer from nucleotides to the dye for the EB/HP1 complex in aqueous solution is 0.16. Similar N and Q_{da} values were obtained previously for a complex of EB with phage DNA (*18*).

On the contrary, no nucleotide band at 260 nm was detected in the excitation spectrum of the Hoechst/HP1 complex. The N and Q_{da} values are equal to zero (Table 3). There is no energy transfer in this non-intercalative complex (but a considerable increase in the own Hoechst emission after its binding to HP1 was observed). The absence of energy transfer indicates that the distance between Hoechst and the nucleotide chromophores are large and/or that the orientation is not coplanar.

Table 3. **Efficiency of energy transfer from nucleotides to dyes.**[a]

Complex	F_d (%)	Q_{da}	N
7AAMD/HP1	~0	~0	~0
Hoechst/HP1	0	0	0
Ethidium/HP1	95	0.16	1.0
7AAMD/λDNA	0.03	0.003	0.06
Hoechst/λDNA	0	0	0
Ethidium/λDNA	–	0.15	1.3

[a]The intensity of the dye excitation band (F_a) was taken as 100%. F_d is the intensity of the donor nucleotide band in the acceptor dye excitation spectrum, Q_{da} is the maximal total energy transfer efficiency from nucleotides to dye, and N is the number of nucleotides donating the energy to one dye molecule. The nucleotide/dye ratio [d]/[a] was 20. Emission of Hoechst was detected at 460 nm, of EB at 610 nm, and of 7AAMD at 640 nm.

Similarly, no nucleotide band was detected at 260 nm in the excitation spectrum of the 7AAMD/HP1 complex. The N and Q_{da} are approximately equal to zero (Table 3), *i.e.* there is no effective energy transfer. This fact is a potent proof against stacking of 7AAMD in HP1. Indeed, this fact is direct evidence that the chromophore of 7AAMD is located far from the nucleotide hetero-cycles and/or has another orientation. Since only one 7AAMD molecule can bind to a single HP1 molecule, N and Q_{da} should be concentration independent.

In the case of the complex of 7AAMD with DNA, the Q_{da} value was 0.003 and N was 0.06 (Table 3), *i.e.* only very little energy transfer was detected. The nucleotide band at 260 nm in the excitation spectrum of the 7AAMD/DNA complex was negligible (*11*, *12*). Energy transfer was absent for Hoechst as well, but not for EB. Thus, it can be stated that the chromophore of 7AAMD does not intercalate into the DNA duplex in a stacking manner between nucleotides, *i.e.* it is non-stacking binding. Anyway, the 7AAMD fluorescence arises mostly from hairpin-like sites and loops. It should be noted here that the efficiency of the energy migration between nucleotides in DNA and HP1 (in aqueous solution) is about zero (*11*, *12*, *19*, *20*). The absence of energy migration along a polynucleotide chain is very important for correct calculation of N and Q_{da}.

The Size of the 7AAMD/HP1 Complex—The effective volume (V) and hydrodynamic length (diameter d) of the 7AAMD/HP1 complex were determined using the Levshin-Perrin equation, and the polarization and lifetime data obtained in our experiment. The lifetime of 7AAMD in the complex with HP1 was 1.7 ns and the polarization was 0.39. These values coincide with our previous data obtained under similar experimental conditions (*12*, *16*). Thus, the V value of the 7AAMD/HP1 complex is ~22,800 Å^3. The d value of the complex is therefore ~35 Å. In the case of free 7AAMD the V value is 4,400 Å^3 and d is 20.3 Å. The ratio of the volumes of the complex and single 7AAMD is 5.2. This value is smaller than the ratio between the molecular weights of the complex and free 7AAMD,

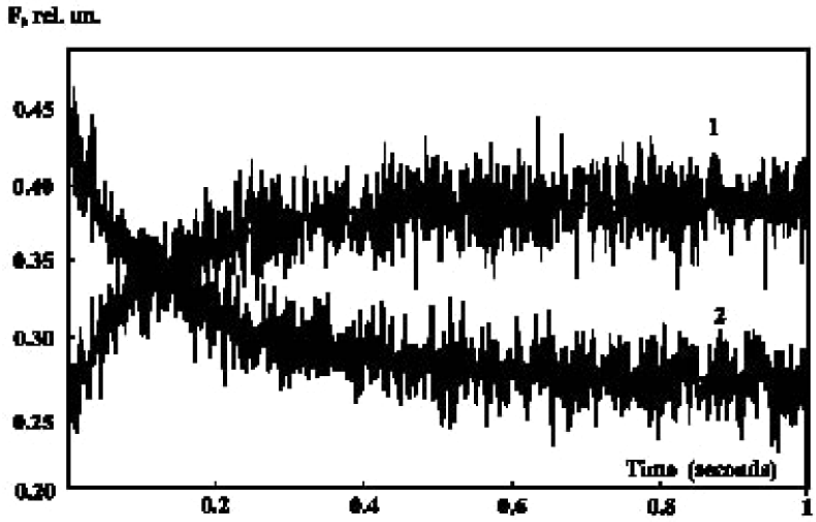

Fig. 2. **Stopped-flow kinetics of binding of 7AAMD to HP1 (1), and substitution of 7AAMD in the 7AAMD/HP1 complex after addition of AMD (2).** Excitation was at 550 nm. The concentrations were: 7AAMD 2 μM, HP1 10 μM, and AMD 10 μM. The buffer was 10 mM Tris-HCl containing 0.5 mM EDTA (pH 7.6). The temperature was 26.3°C.

which is 7.4. The observed discrepancy between the two mentioned volumes may be due to that 7AAMD is located in the cavity inside HP1 (not on the surface of HP1).

Prompt Binding of 7AAMD and AMD with HP1—Using stopped-flow fluorimetry, Chen *et al.* (*24*) observed two components in the 7AAMD fluorescence kinetics during its dissociation from short hairpin-like oligonucleotides in the presence of a detergent. Dissociation of 7AAMD from hairpin structures was considered to be a fast process, whereas dissociation from duplex DNA was assumed to be a slow process.

The formation of the complex between HP1 and 7AAMD is a prompt process. It is much faster than the first component of 7AAMD binding to DNA. In the stopped-flow experiments, it was found that the kinetics of binding of 7AAMD to HP1 (Fig. 2) consist only of the fast single component. The characteristic time of the 7AAMD/HP1 complex formation is about 0.3 s (Table 4). No slower component was observed. The emission spectrum and lifetime of 7AAMD in the 7AAMD/HP1 complex were almost the same as those for 7AAMD in pyridine (*16*). This constitutes evidence that the binding of 7AAMD to the outer surface of HP1 is uncertain. The binding process seems to comprise rapid penetration of 7AAMD into a hydrophobic cavity inside HP1, but not the stacking intercalation of 7AAMD between the planes of nucleotides. The 7AAMD molecule might be located inside the HP1 cavity between adenine and thymine bases without stacking-like intercalation.

To study the competition between 7AAMD and AMD for the binding site in HP1, excess AMD was added to the 7AAMD/HP1 complex. The fluorescence intensity decreased immediately after the addition (Table 2). Consequently, 7AAMD was completely replaced in the complex by AMD. The replacement of 7AAMD by AMD is a very fast process. The characteristic time is about 0.3 s (Fig. 2). The time of replacement of 7AAMD by AMD is the same as the characteristic time of the binding of 7AAMD to HP1. Thus, one can conclude, that there is no energy barrier for substitution of 7AAMD by AMD in the complex with HP1 and *vice versa*. Similar (but not so pronounced) competition between 7AAMD and AMD was also observed in DNA (Table 2).

Table 4. **Fast and slow components of 7AAMD or AMD binding to HP1 and λDNA, calculated from changes in the 7AAMD emission kinetics.**[a]

Sample	t_1 (s)	t_2 (s)	a_2/a_1
7AAMD + HP1	0.3*	–	–
7AAMD and HP1 + AMD	0.3*	–	–
7AAMD + DNA	4.6	40	0.3
7AAMD and HP1 + DNA	4.5	101	1.7
7AAMD, NaCl and HP1 + DNA	4.9	147	3.5

[a]The concentrations used: 7AAMD 1 μM, HP1 2.4 μM (*i.e.* 0.021 mg/ml), λDNA 0.014 mg/ml, and NaCl 50 mM. The buffer was 20 mM Tris-HCl containing 1 mM EDTA (pH 7.5). Excitation and emission were at 570 and 610 nm. In the two upper stopped-flow experiments the concentrations were: 7AAMD 2 μM, HP1 10 μM, and AMD 10 μM; excitation was at 550 nm, and emission was detected at >570 nm. The values of t_1, t_2, a_1, and a_2 were obtained by kinetic data fitting.

Binding of 7AAMD with λDNA—It is well known that the binding kinetics of 7AAMD or AMD interaction with DNA are biphasic: fast (ms/s) and slow (minutes) processes take place (*24–27*). Figure 3 shows the emission kinetics of 7AAMD binding to an excess of native λDNA. The experimental kinetics are described by at least two components: with characteristic times of 4.6 s and 40 s (Table 4). The first component exhibits the higher amplitude (slow to fast component ratio a2/a1 is 0.3). Since λDNA is relatively short, it has almost no breaks. It can be suggested that the fast component corresponds to the binding of 7AAMD inside loops and single strand areas, whereas the slow component corresponds to penetration of 7AAMD into the double helix.

The duration of the first component in the case of λDNA was one order of magnitude longer than that for HP1. This reflects the fact that hairpin-like sites and loops in λDNA are compact rigid structures, whereas the HP1 hairpin is flexible and loosened. In the case of λDNA, the slow component corresponds to not only slow embedding of 7AAMD into a double helix, but also dilatory binding of 7AAMD with, due to thermal fluctuations, dynamically slow appearing hairpin-like sites and loops in the long DNA molecule.

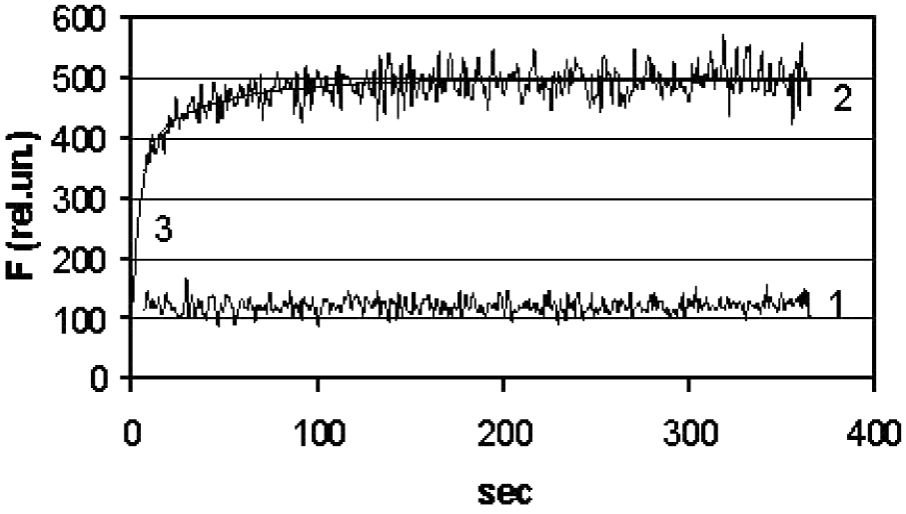

Fig. 3. **The kinetics of 7AAMD binding to lambda DNA (2), its fitting (3), and 7AAMD without DNA (1).** Excitation was at 570 nm, and emission was at 610 nm. The concentrations were: 7AAMD 1 μM, and λDNA 0.014 mg/ml. The buffer was 20 mM Tris-HCl (pH 7.6).

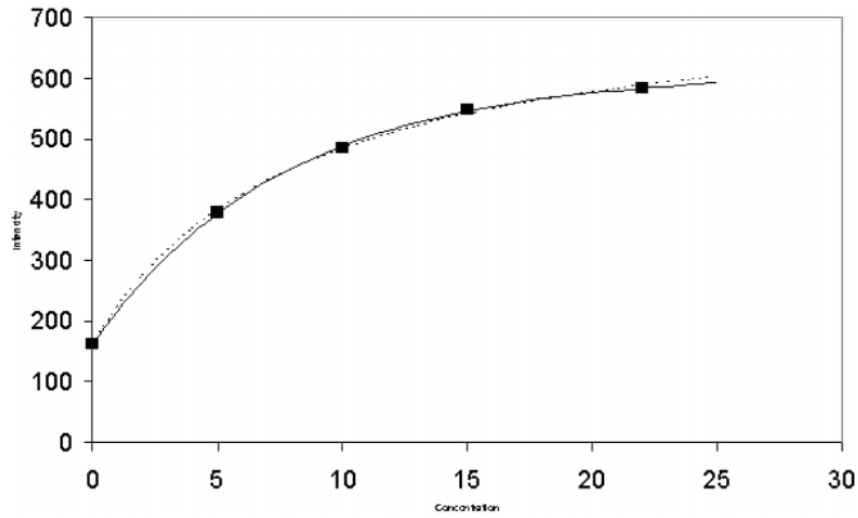

Fig. 4. **Intensity of the 7AAMD emission (at plateau) depending on the λDNA concentration (μM nucleotides).** The temperature was 20°C. Excitation was at 570 nm, and emission at 610 nm. The concentration of 7AAMD was 1 μM. The buffer was 20 mM Tris-HCl containing 1 mM EDTA (pH 7.5).

The rate of binding to DNA and the equilibrium fluorescence intensity of 7AAMD depend on the DNA concentration in solution. The Fig. 4 shows that λDNA at concentrations of 5–10 μM of bases is unable to bind whole 1 μM 7AAMD. The 7AAMD emission achieves a plateau at a concentration of ~22 μM of bases (*i.e.* 7 μg/ml; the molecular weight of λDNA is 32×10^6). At this concentration, λDNA binds 99% of 1 μM 7AAMD, *i.e.* the nucleotide/7AAMD ratio is ~22. This means that native λDNA in aqueous solution (in buffers of low ionic strength, without salts) can form one hairpin-like site or loop every 37 Å of double helix.

Slow Redistribution of 7AAMD from HP1 to DNA—The phenoxazone chromophore of 7AAMD or AMD is located in DNA molecules in a hydrophobic environment (*12, 16*). The fluorescence quantum yield of 7AAMD highly increases after 7AAMD binds to HP1, but not so highly when 7AAMD binds to DNA (Table 2). This means that photo-excited 7AAMD molecules are quenched by nucleotides in DNA stronger than in HP1. This fact allows observation of the redistribution of 7AAMD from HP1 to DNA. Indeed, a considerable decrease in the 7AAMD emission during incubation of the 7AAMD/HP1 complex with DNA was detected (Fig. 5). Consequently, 7AAMD is transferred from HP1 to DNA after addition of DNA to the 7AAMD/HP1 complex. Rapid and slow phases in this process were observed. At high concentrations of λDNA, the redistribution kinetics were fitted by a two-component model with characteristic times of 4.5 s and 101 s; the amplitude ratio a_2/a_1 was 1.7 (Table 4). The fluorescence changes caused by the slow component were larger. The first component has almost the same duration as in the case of direct binding of 7AAMD to DNA. The second component has a 2.5 times longer characteristic time compared to direct binding of 7AAMD to DNA. The process of redistribution was faster with increasing DNA concentration. The two detected components might correspond to the two different DNA sites to which 7AAMD is transferred. The increase in ionic strength (50 mM NaCl) leads to a 1.8-fold decrease in the amplitude of the fast component, whereas the slow component does not change much. Ionic interactions control the rate of 7AAMD redistribution from HP1 to DNA due to the well known conformational transition of a loosened DNA in water without salts to a more rigid compact DNA at high ionic strength.

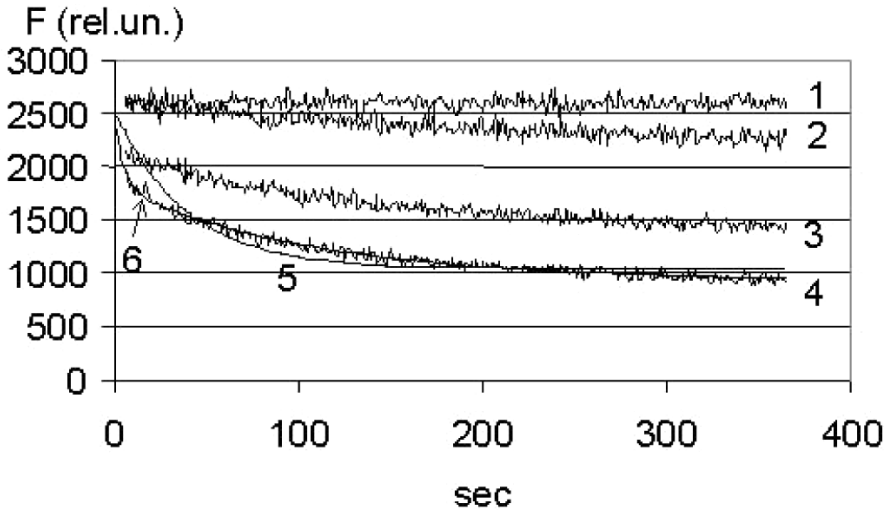

Fig. 5. **Emission kinetics for redistribution of 7AAMD from HP1 to λDNA (with various λDNA concentrations).** Concentrations of λDNA were 0.0 (1), 0.0035 mg/ml (2), 0.007 mg/ml (3), and 0.014 mg/ml (4). The concentration of 7AAMD was 1 μM, HP1 0.021 mg/ml. The buffer was 20 mM Tris-HCl (pH 7.6). Excitation was at 570 nm, and emission at 610 nm. The curves for a one-exponential model (5) and a two-exponential model (6) are shown.

HP1 acts as a protecting coat for 7AAMD or AMD. But this coat does not prevent the penetration of actinomycins into DNA. Perhaps hairpin oligonucleotides could be tested for medicines like molecular carriers of antibiotics.

The authors are grateful to Dr. R. Wadkins (USA) and I. Savintsev (Russia) for the useful discussions and kind assistance, and to CRDF and NATO for the financial support of two fellowships in the USA.

REFERENCES

1. Kaji, T., Takamatsu, H., Noguchi, H., Tahara, H., Adachi, Y., Kajiya, H., Kawakami, K., Nomoto, S., and Satou, E. (1999) Yolk sac tumour of the ovary in a conjoined twin. *Eur. J. Pediatr. Surg*. **7**, 311–312
2. Shen, K., Lang, J., and Huang, H. (2001) Treatment of childhood genital malignancies. *Zhonghua Fu Chan Ke Za Zhi.* **36**, 360–363
3. Ducrey, N., Nenadov-Beck, M., and Spahn, B. (2002) Update of orbital rhabdomyosarcoma therapy in children. *J. Fr. Ophtalmol.* **25**, 298–302
4. Sokolov, T., Stoianova, A., Mumdjiev, I., and Mihova, A. (2001) Treatment of Ewing's sarcoma with 2 different protocols. *Ann. Med. Interne* **152**, 497–501
5. Frolkis, V.V. (1988) *Aging and Increase of Life Expectancy* (in Russian), Leningrad, USSR
6. Muller, W. and Crothers, D.M. (1975) Interactions of heteroaromatic compounds with nucleic acids: the influence of heteroatoms and polarizability on the base specificity of intercalating ligands. *Eur. J. Biochem.* **54**, 267–77
7. Gurski, V. (1969) Structure of DNA-actinomycin complexes. *Mol. Biol. (Moscow)* **3**, 749–756
8. Krivtsova, M.A, Moroshkina, E.B., Hamman, H., Glibin, E.N., and Frisman, E.V. (1981) Study of interaction of DNA with small-molecular ligands of various structure. *Mol. Biol. (Moscow)* **15**, 613–621
9. Robinson, H., Gao, Y.-G., Yang, X.-L., Sanishvili, R., Joachimiak, A., and Wang, A.H.-J. (2001) Crystallographic analysis of a novel complex of actinomycin D bound to the DNA decamer CGATCGATCG. *Biochemistry* **40**, 5587–5592
10. Snyder J.G. (1989) Binding of actinomycin D to DNA: evidence for a nonclassical high-affinity binding mode that does not require GpC sites. *Proc. Natl. Acad. Sci. USA* **86**, 3968–3972
11. Savintsev, I.V. and Vekshin, N.L. (2004) Formation of complexes of actinomycins with DNA in solutions and films. *Appl. Biochem. and Microbiol. (Moscow)* **41**, 1–8
12. Savintsev, I.V. and Vekshin, N.L. (2002) Binding sites for 7-amino-actinomycin D and actinomycin D in DNA and model nucleotide systems. *Mol. Biol. (Moscow)* **36**, 725–730
13. Wadkins, R.M. and Jovin, T.M. (1991) Actinomycin D and 7-aminoactinomycin D binding to single-stranded DNA. *Biochemistry* **30**, 9469–9478
14. Wadkins, R.M., Vladu, B., and Tunng, C. (1998) Actinomycin D binds to metastable hairpins in single-stranded DNA. *Biochemistry* **37**, 11915–11923
15. Wadkins, R.M., Tunng, C., Vallone, P.M., and Benight, A.S. (2000) The role of the loop in binding of an actinomycin D analog to hairpins formed by single-stranded DNA. *Arch. Biochem. Biophys.* **384**, 199–203
16. Vekshin, N., Savintsev, I., Kovalev, A., Yelemessov, R., and Wadkins, R. (2001) Solvatochromism of the excitation and emission spectra of 7-aminoactinomycin D: implications for drug recognition of DNA secondary structures. *J. Phys. Chem. B* **105**, 8461–8467
17. Kovalev, A.E., Yakovenko, A.A., and Vekshin, N.L. (2004) Investigation of 7-amino-actinomycin D and DNA by fluorescence correlated microscopy. *Biophysics (Moscow)* **49**, 1030–1037
18. Vekshin, N.L. (1998) Migration of energy in DNA, estimated by fluorescence of intercalating dye. *J. Appl. Spectrosc. (Russia)* **65**, 794–798
19. Vekshin, N.L. (2002) *Photonics of Biopolymers*, Springer, Berlin
20. Vekshin, N.L. (1999) Screening hypochromism in molecular aggregates and biopolymers. *J. Biol. Phys.* **25**, 339–354
21. Sha, F. and Chen, F.M. (2000) Actinomycin D binds strongly to d(CGAGACG) and d(CGTCGTCG). *Biophys. J.* **79**, 2095–2104
22. Vekshin, N.L. (1997) *Energy Transfer in Macromolecules*, SPIE, Bellingham
23. Saito, M., Kobayashi, M., Iwabuchini, S.-I., Morita, Y., Takamura, Y., and Tamiya, E. (2004) DNA condensation monitoring after interaction with Hoechst 33258 by atomic force microscopy and fluorescence spectroscopy. *J. Biochem.* **136**, 813–823
24. Chen, F.M., Jones, C.M., and Johnson, Q.L. (1993) Dissociation kinetics of actinomycin D from oligonucleotides with hairpin motifs. *Biochemistry* **32**, 5554–5559
25. Bittman, R. and Blau, L. (1975) Stopped-flow kinetic studies of actinomycin binding to DNAs. *Biochemistry* **14**, 2138–2145
26. Brown, S.C. and Shafer, R.H. (1977) Kinetic studies of actinomycin D binding to mono-, oligo-, and polynucleotides. *Biochemistry* **26**, 277–282
27. Fox, K.R. and Waring, M.J. (1984) Kinetic evidence for redistribution of actinomycin molecules between potential DNA-binding sites. *Eur. J. Biochem.* **145**, 579–586